Conference Applications of Mathematics 2013
in honor of the 70th birthday of Karel Segeth.
Jan Brandts, Sergey Korotov, Michal Křížek,
Jakub Šístek, and Tomáš Vejchodský (Eds.),
Institute of Mathematics AS CR, Prague 2013

RIEMANN SOLUTION FOR HYPERBOLIC EQUATIONS WITH DISCONTINUOUS COEFFICIENTS

L. Remaki

BCAM – Basque Centre for Applied Mathematics
Mazarredo 14, 48009 Bilbao, Basque Country, Spain
lremaki@bcamath.org

Abstract

This paper deals with a Riemann solution for scalar hyperbolic equations with discontinuous coefficients. In many numerical schemes of Godunov type in fluid dynamics , electromagnetic and so on, usually hyperbolic problems are solved to estimate fluxes. The exact solution is generally difficult to obtain, but good approximations are provided in many situations like Roe and HLLC Riemann solvers in fluid. However all these solvers assumes that the acoustic waves speeds are continuous which is not true as we will show in this paper. A new Riemann solver is then proposed based on previous work of the author and an application to a gas-particle model for a 90 degree curved bend is performed.

1. Introduction

In many numerical methods such as the dual-mesh finite volume, DG methods, estimation of convective numerical fluxes at the (dual) interfaces is required. The accuracy of the method depends on the accuracy of the flux estimation. The most popular methods consists of using a Riemann approximation solver, because of its physical meaning. This approach was proposed first by Godunov [3] and then many Riemann solver approximations where developed. The most popular being Roe solver [8, 9] where the Jacobian matrix is averaged in such way that hyperbolicity, consistency with the exact Jacobian and conservation across discontinuities are fulfilled. For fluid application this solver has been modified [1, 2] to overcome the shortcoming for low-density flows. HLL Riemann solver [4] proposed to solve for the original flux, the major drawback of this solver due to the space averaging process, is that contact discontinuities, shear waves and material interfaces are not captured. To remedy to this problem, the HLLC solver [10] was proposed, by adding the missing wave to the structure. However, all these methods assume that the waves speeds are continuous through the interfaces (intercellular in the case of finite volume dual mesh) by applying diverse averaging process. This is not true in reality; typical situations are recirculation for turbulent flows and transitions from subsonic to supersonic for transonic regimes. To remedy to this situation and as a first step

a Riemann solver of scalar hyperbolic linear equation with discontinuous coefficient is developed, this is based on a first idea developed in [7]. This solver takes into account the discontinuities of waves speeds and shows physical behaviours that are missed by the existing solvers. Numerical proof of the proposed solution is provided and an application to a gas-particle model with a validation against experimental results for a 90^0 curved bend described in [5] is performed.

2. *Riemann* solution for hyperbolic equation with discontinuous coefficient

Consider the following scalar linear hyperbolic equation with discontinuous coefficient,

$$\begin{aligned} \tfrac{\partial}{\partial t}\varphi + \beta(x)\tfrac{\partial}{\partial x}\varphi = 0 \qquad & \text{on } \Omega \times [0,T]\,, \\ \varphi(0,x) = \varphi^0 = \begin{cases} \varphi_L & \text{if} \quad x < 0\,, \\ \varphi_R & \text{if} \quad x > 0\,, \end{cases} & \\ \beta(x) = \begin{cases} \beta_L & \text{if} \quad x < 0\,, \\ \beta_R & \text{if} \quad x > 0\,, \end{cases} & \end{aligned} \tag{1}$$

In this equation, the acoustic wave speed β is discontinuous which is not taken into account in the existing *Riemann* solvers, where acoustic waves speeds are assumed to be continuous in the vicinity of the origin. To build a solution let us first analyze the following different situations.

Case 1: $\beta_L > 0$ and $\beta_R > 0$ we have propagation of the discontinuity (of initial condition) to the right and we do not need to consider what happening within the fan defined by the two acoustic waves, because they will catch up if $\beta_L > \beta_R$ and if $\beta_L < \beta_R$ an expansion will appear.

Case 2: $\beta_L < 0$ and $\beta_R < 0$ similar the previous case with a propagation of the discontinuity to the left.

Case 3: $\beta_L < 0$ and $\beta_R > 0$ we have propagation of the discontinuity to the left and the right simultaneously, and we need to determine what happened within the fan defined by the two acoustics waves. We assume that a constant state appears and its expression will be given below.

Case 4: $\beta_L > 0$ and $\beta_R < 0$ in this case we have opposite acoustic wave speeds and then the discontinuity will remain blocked, which means there is no propagation.

Based on the above analysis, the *Riemann* solution of problem (4) is given by

$$\varphi(x,t) = \begin{cases} \varphi_L & \text{if} \quad \beta_L > 0 \quad \text{and} \quad \beta_R > 0, \\ \lambda & \text{if} \quad \beta_L < 0 \quad \text{and} \quad \beta_R > 0, \\ \varphi_R & \text{if} \quad \beta_L < 0 \quad \text{and} \quad \beta_R < 0, \\ \varphi^0 & \text{if} \quad \beta_L > 0 \quad \text{and} \quad \beta_R < 0, \end{cases} \tag{2}$$

where the expression of the constant λ is given by

$$\lambda = \frac{\frac{1}{\beta_L}\varphi_L + \frac{1}{\beta_R}\varphi_R}{\frac{1}{\beta_L} + \frac{1}{\beta_R}} \tag{3}$$

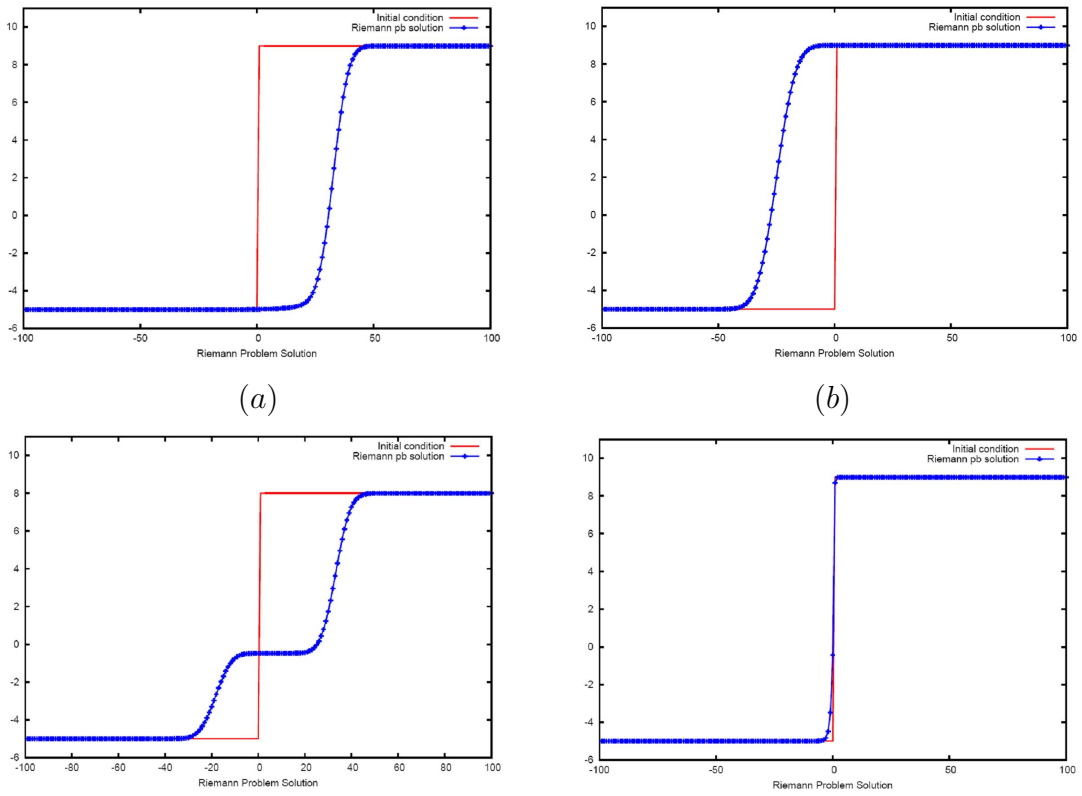

Figure 1: Initial condition and Riemann solution after 100 time iterations: a) Case 1, b) Case 2, c) Case 3, d) Case 4.

To prove solution (2) and formula (3) at least numerically, the *Riemann* problem (1) is solved using a centred finite volume scheme stabilized with a first order artificial viscosity, which is equivalent in this case to a finite difference scheme. Several initial conditions φ^0 and acoustic wave β values are tested. All tests confirm the proposed solution, two examples are shown in Figures 1 and 3. We can see in particular the solutions corresponding to cases 3 and 4, it is clear that they could not be obtained if the coefficient β is averaged as in the existing *Riemann* solvers. Figures 2 and 4 show the perfect agreement of the proposed analytical expression of λ with the predicted numerical value.

3. Application to gas-particle model discretization

In this section the proposed Riemann solver is applied to discretize part of gas-particle model that describes a motion of particles under the effect fluid drag forces. A 90 degree bend is then simulated and results are compared to experimental data. First let us recall equations governing three-dimensional unsteady viscous compressible flow coupled with a particle motion equation in Eulerian modelisation:

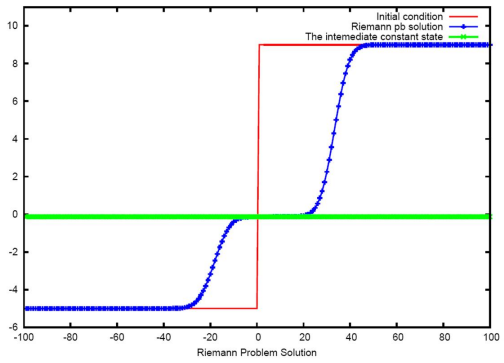

Figure 2: Initial condition and Riemann solution corresponding to Case 3 and the analytical value of λ.

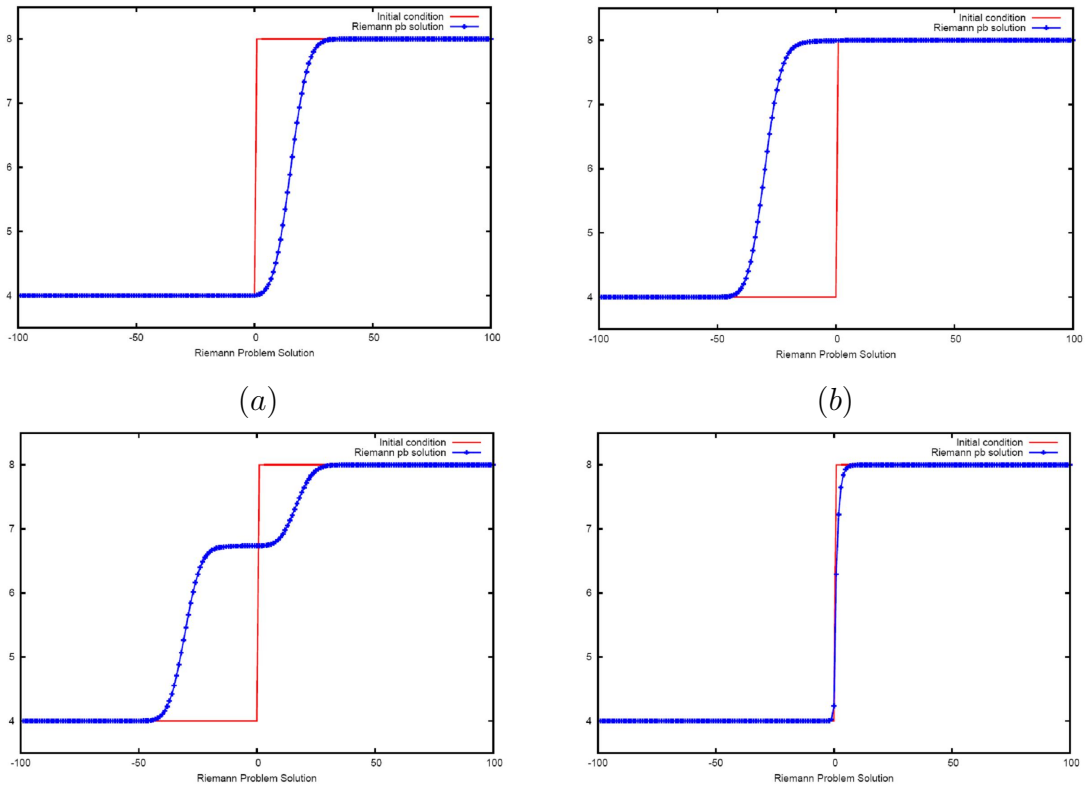

Figure 3: Initial condition and Riemann solution corresponding to Case 3 and the analytical value of λ.

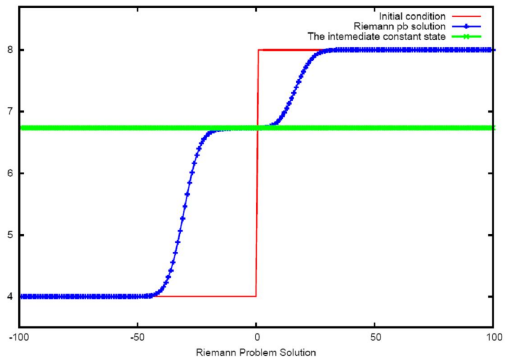

Figure 4: (a) Riemann Solution: a) Initial condition, b) Solution after 100 time iterations.

Fluid phase:

$$\frac{\partial}{\partial t}(\phi_g \rho_g) + \nabla(\phi_g \rho_g U_g) = 0 \qquad \text{on } \Omega \times [0,T] \ , \tag{4}$$

$$\frac{\partial}{\partial t}(\phi_g \rho_g U_g) + \nabla(\phi_g \rho_g U_g \otimes U_g) = -\nabla P_g + \nabla \tau_g - d_{fac} \frac{1}{\tau_p} \phi_g (U_g - U_p) \qquad \text{on } \Omega \times [0,T] \ . \tag{5}$$

Gas phase:

$$\frac{\partial}{\partial t}(\phi_p \rho_p) + \nabla(\phi_p \rho_p U_p) = 0 \qquad \text{on } \Omega \times [0,T] \tag{6}$$

$$\frac{\partial}{\partial t}(\phi_p \rho_p U_p) + \nabla(\phi_p \rho_p U_p \otimes U_p) = -\frac{\phi_p}{\rho_p} \nabla P_g + d_{fac} \frac{1}{\tau_p} \phi_p (U_g - U_p) + \phi_p (1 - \frac{\rho_g}{\rho_p}) \qquad \text{on } \Omega \times [0,T] \ , \tag{7}$$

where ϕ_g and ϕ_p are the gas and particle volume fraction satisfying the conservation condition $\phi_g + \phi_p = 1$, $d_{fac} = \begin{cases} 1 + 0.15 R_{e_0}^{0.687} & \text{if } R_{e_0} < 1000 \\ 0 \quad \text{else} \end{cases}$ is the drag coefficient, $R_{e_0} = \frac{D_p |U_p - U_g|}{\nu_g}$ is the particle Reynolds number, $\tau_p = \frac{\rho_p D_p^2}{18 \mu_g}$ is the particle response time and $\overrightarrow{g}$ is the gravity.

In this model only Drag and gravity forces are considered in the particle-gas interaction.

3.1. Numerical discretization

A finite volume method is used to discretize the overall gas-particle model. In the solid phase, the particle fraction volume variable vanishes, where the sand is absent which results in dividing by zero when computing the velocity vector in equation (7). This leads obviously to a severe instability of the scheme. To avoid this situation the non-conservative form of the momentum equation is considered, while the conservative form of the volume fraction is kept. The momentum equation takes the form:

$$\frac{\partial}{\partial t}(U_p) + \nabla(U_p \otimes U_p) = -\frac{1}{\rho_p}\nabla P_g + d_{fac}\frac{1}{\tau_p}(U_g - U_p) + (1 - \frac{\rho_g}{\rho_p}) \quad \text{on } \Omega \times [0, T]. \tag{8}$$

The inviscid fluxes of the fluid phase are estimated using a second order HLLC *Riemann* solver and the limiter developed in [6]. For the solid phase a centered scheme is used for the non-conservative momentum equations of the solid phase, and it is stabilized by adding a first order artificial viscosity of the form

$$\triangle Q_i = \sum_{J \in N_I} \lambda_{IJ} \left(Q_J - Q_I\right). \tag{9}$$

With $\lambda_{IJ} = \frac{1}{1+\tan(\theta_{IJ})^2}$, and θ_{IJ} is the angle between the normal to the surface η_I and the velocity vector U_I. This allows diffusion to act mostly in the flow direction while minimizing the cross wind effects similar to streamline diffusion methods.

To estimate the volume fraction flux in the solid phase, we need to solve a *Riemann* problem of a hyperbolic equation with discontinuous coefficient of the type $\frac{\partial}{\partial t}(\phi_p) + q_{IJ}\frac{\partial}{\partial s}(\phi_p) = 0$, where $q_{IJ} = U_p^I \eta_{IJ}$ and U_p^I is the particle velocity at node I and η_{IJ} is the normal to the surface separating dual cells associated with nodes I and J. To take into account of such discontinuities, the proposed *Riemann* solver is used.

3.2. Validation

The numerical model is validated against experimental results of a 90° bend test case described in [5]. This test case was selected first because of the availability of experimental data and then for the wide use of curved ducts in industrial applications such as air-coal flows in coal combustion equipments, coal liquefaction-gasification pipe systems, gas-particle flows in turbo machinery, and contaminant particle flows in ventilation ducts. The apparatus and geometry of the test are shown on figure 5 scanned from reference [5]. The 90° duct has a square cross-section of $D = 0.1\,\text{m}$ and upstream and downstream duct lengths are 1 m and 1.2 m, respectively. Glass spherical particles with a material density of $2990\,\text{kg/m}^3$ and diameter size of $50\,\text{kg/m}^3$ are used. The inlet fluid and particles velocity is set to $52.19\,\text{m/s}$, for more details see [5]. For the numerical simulation a hybrid mesh is used as shown in Figure 6. The mesh contains 766614 tetrachordal elements and 1229952 prisms forming 12 boundary layers. The computational domain starts $10D$ upstream from the bend entrance

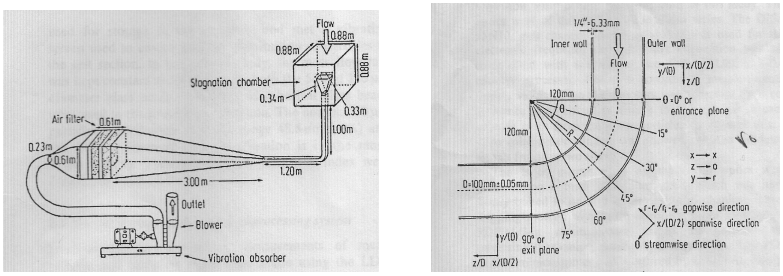

(a) (b)

Figure 5: Experimental apparatus: (a) General flow system, (b) Geometry of the curved square duct.

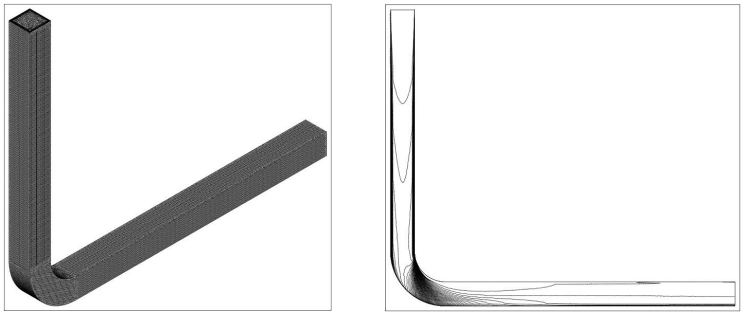

Figure 6: Hybrid used mesh and volume fraction profile for the curved duct.

and extends up to $12D$ downstream from the bend exit. The classical viscous flow boundary condition are imposed for the the fluid phase while a rebounding particle-wall conditions with normal and tangential restitution coefficients of 0.9 and 0.8 respectively, are considered for the solid phase. Finally, the turbulence features are captured using the Spalart-Allmaras turbulent model.

3.3. Results

Figure 6 shows the used mesh and the particles volume fraction profile. Figure 7 shows the residual convergence to the steady state. Figure 8 shows a good agreement of the fluid and particles mean stream velocity with experimental results for the different sections shown in 5-(b). This demonstrates the validity and the accuracy of the physical and numerical model.

4. Conclusions

The paper presented a new *Riemann* solver for scalar hyperbolic equations with discontinuous coefficient. A numerical proof of physical phenomena predicted by the proposed solver and missed by all existing *Riemann* solvers is provided. Appli-

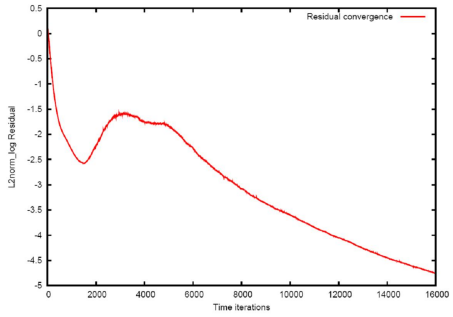

Figure 7: Bend case: Residual convergence.

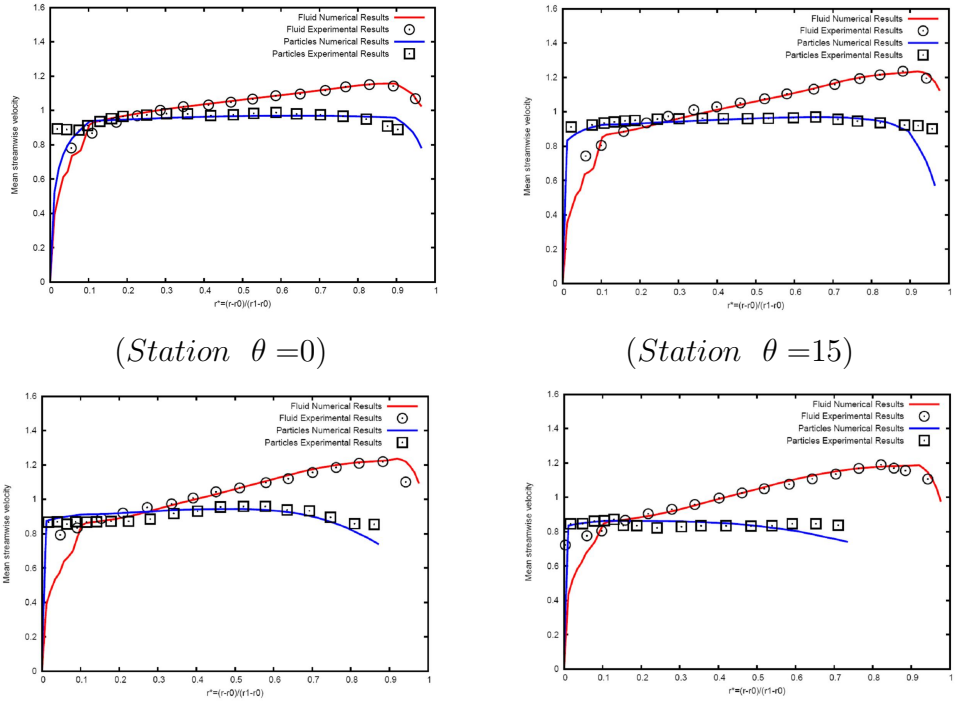

(*Station* θ =0) (*Station* θ =15)

(*Station* θ =30) (*Station* θ =45)

Figure 8: 90 Bend case: Mean Stream fluid and particles velocity comparison to experimental results for different stations.

cation of the solver in a gas-particle model discretization is achieved and applied to a 90 curved bend with comparison to experimental data. This work is a first step toward a construction of a *Riemann* solver for systems with discontinuous coefficients and its application for inviscid fluxes estimation in the Navier-Stokes and electromagnetic equations discretization.

References

[1] Einfeldt, B.: On gudonov-type methods for gas dynamics. SIAM J. Numer. Anal. **25**(2) (1988), 294–318.

[2] Einfeldt, B., Munz, C., Roe, P., and Sjgreen, B.: On Gudonov-type methods near low densities. J. Comput. Phys. **92** (1991), 273–295.

[3] Godunov, S.: A finite difference method for the computation of discontinuous solutions of the equations of fluid dynamics. Comp. Math. (in Russian) **47** (1959), 357–393.

[4] Harten, A., Lax, P., and Van Leer, B.: On upstream diffrencing and Gudonov-type schemes for hyperbolic conservation laws. SIAM Review **25**(1) (1983), 35–61.

[5] Kliafas, Y. and Holt, M.: LDV measurements of a turbulent air-solid two-phase flow in a 90° bend. Experiments in Fluids **5** (1987), 73–85.

[6] Remaki, L., Hassan, O., and Kenneth, K.: New limiter and gradient reconstruction method for HLLC-finite volume scheme to solve Navier-Stokes equations. In: *TECCOMAS, the fifth European Congress on Computational in Fluid Dynamic, Lisbon, Portugal.*, 14–17 June 2010.

[7] Remaki, L.: Theoretical and numerical study of quasi-linear equations with discontinuous coefficients, and 2D linear acoustic. PhD Thesis, 1997, France.

[8] Roe, P.: Approximate riemann solvers, parameter vectors, and difference schemes. J. Comput. Phys. **43** (1981), 357–372.

[9] Roe, P.: Characteristic-based schemes for the Euler equations. Ann. Rev. Fluid Mech. **18** (1986), 337.

[10] Toro, E., Spruce, M., and Spearses, W.: Restoration of the contact surface in the HLL Riemann solver. Shock Waves **4** (1994), 25–34.